European Journal of Pharmaceutics and Biopharmaceutics 134 (2019) 166–177

Contents lists available at ScienceDirect

European Journal of Pharmaceutics and Biopharmaceutics

journal homepage: www.elsevier.com/locate/ejpb

Research paper

Solid lipid nanoparticles for the delivery of anti-microbial oligonucleotides

Ana González-Paredes[a,*], Leopoldo Sitia[b,c,1], Angels Ruyra[d], Christopher J. Morris[e], Grant N. Wheeler[d], Michael McArthur[b,c], Paolo Gasco[a]

[a] Nanovector Srl., Via Livorno 60, 10144 Turin, Italy
[b] Procarta Biosystems Ltd., Innovation Centre, Norwich Research Park, Norwich NR4 7UH, UK
[c] Norwich Medical School, University of East Anglia, Norwich NR4 7UQ, UK
[d] School of Biological Sciences, University of East Anglia, Norwich NR4 7TJ, UK
[e] School of Pharmacy, University of East Anglia, Norwich NR4 7TJ, UK

ARTICLE INFO

Keywords:
Oligonucleotide
Antibacterial
Transcription factor decoy
Solid lipid nanoparticles
Intracellular delivery

ABSTRACT

Novel alternatives to antibiotics are urgently needed for the successful treatment of antimicrobial resistant (AMR) infections. Experimental antibacterial oligonucleotide therapeutics, such as transcription factor decoys (TFD), are a promising approach to circumvent AMR. However, the therapeutic potential of TFD is contingent upon the development of carriers that afford efficient DNA protection against nucleases and delivery of DNA to the target infection site. As a carrier for TFD, here we present three prototypes of anionic solid lipid nanoparticles that were coated with either the cationic bolaamphiphile 12-bis-tetrahydroacridinium or with protamine. Both compounds switched particles zeta potential to positive values, showing efficient complexation with TFD and demonstrable protection from deoxyribonuclease. The effective delivery of TFD into bacteria was confirmed by confocal microscopy while SLN-bacteria interactions were studied by flow cytometry. Antibacterial efficacy was confirmed using a model TFD targeting the Fur iron uptake pathway in *E. coli* under microaerobic conditions. Biocompatibility of TFD-SLN was assessed using *in vitro* epithelial cell and *in vivo Xenopus laevis* embryo models. Taken together these results indicate that TFD-SLN complex can offer preferential accumulation of TFD in bacteria and represent a promising class of carriers for this experimental approach to tackling the worldwide AMR crisis.

1. Introduction

Antimicrobials have been a marked success in modern medicine, greatly reducing death and morbidity associated with bacterial infections. However, the antibiotic era is widely thought to be coming to an end due to their overuse or misuse in the clinic. Strains of bacteria have developed multiple-drug resistance (MDR) and are no longer treatable [1]. Conventional pharmaceutical approaches have failed to discover any new class of antimicrobials for 30 years and there is now a pressing need to develop alternatives to conventional antimicrobials [2,3]. Alternative strategies include oligonucleotide therapeutics that have the advantages of not being susceptible to resistance mechanisms to standard antibiotics and acting on novel therapeutic targets, such as transcription, that up to now have been undruggable. Moreover, targeting non-essential genes should further reduce the possibility of resistance development [4,5]. Due to the large size, high anionic charge and hydrophilic nature of native oligonucleotides (ON) they are unable to cross the membranes of bacteria to reach their targets. Hence the challenge of efficient delivery must be faced to develop ON therapeutics. Optimal delivery systems should encapsulate the ON with high efficiency and protect them from degradation, should not trigger immunogenic reactions in the host and be safe [6]. Typically ON antimicrobials are conjugated with cationic moieties, like cell penetrating peptides (CPP), which are typically cationic and bind readily to bacterial membranes [7]. However, CPP use is limited to highly modified antisense ON, which have neutrally charged backbones, otherwise they would cause negatively charged ON precipitation [8] These conjugates show efficacy in *in vitro* and *in vivo* models of bacterial infections but only at relatively high concentrations, which has limited their development, also due to high cytotoxicity [9,10]. Other interesting cationic

Abbreviations: AMR, antimicrobial resistant; TFD, transcription factor decoys; SLN, solid lipid nanoparticles; ON, oligonucleotide; 12-bis-THA or THA, 1,1′-(dodecane-1,12-diyl)-bis-(9-amino-1,2,3,4-tetrahydroacridinium) chloride; PC, phosphatidylcholine; TFF, tangential flow filtration

* Corresponding author at: Nanovector Srl., Via Livorno 60, 10144 Turin, Italy.
E-mail address: agonzalez@nanovector.it (A. González-Paredes).
[1] Present address: Nanobiointeractions & Nanodiagnostics, Istituto Italiano di Tecnologia (IIT), Via Morego 30, 16163 Genoa, Italy.

https://doi.org/10.1016/j.ejpb.2018.11.017
Received 8 July 2018; Received in revised form 18 November 2018; Accepted 19 November 2018
Available online 20 November 2018
0939-6411/

compound for ON delivery is dequalinium, a well-known drug with antimicrobial activity, which has been described for its ability to form self-assembled structures that efficiently bind DNA and afford high transfection efficiencies in bacteria [11]. In this regard, a recently described bolaamphiphilic molecule with analogous structure, 1,1′-(dodecane-1,12-diyl)-bis-(9-amino-1,2,3,4-tetrahydroacridinium) chloride (12-bis-THA or simply THA), showed a strong affinity towards cardiolipin, which plays an important role in the dynamic organization of bacterial membranes, and effectively delivers ON into *Clostridium difficile* in an animal model [12]. ON and 12-bis-THA form nanoparticles with sizes between 90 and 400 nm depending on the structure of the ON; however, these nanoparticles can be prepared only as a dilute suspension and they showed poor stability in physiological conditions, and moderate cytotoxicity *in vitro* [13].

Solid lipid nanoparticles (SLN) are versatile carriers which can be designed for nucleic acid delivery [14–16], with several advantages: their production is relatively simple and scalable, they have long term stability and they can be sterilized by filtration. Furthermore, SLN can be administered by different routes and show very favorable toxicity profiles. It is even possible to control the release of associated cargo by modification of SLN lipid matrix [16]. As applied in other nucleic acid delivery systems, SLN surfaces can be modified to introduce positive charge and establish electrostatic interaction with negatively charged nucleic acids, so favoring its condensation and penetration into target cells [17], i.e. ON-SLN complexes can be obtained by simple incubation of ON with cationic SLN. ON-SLN-mediated transfection has been previously reported by several researchers, both *in vitro* (eukaryotic cells) [18,19] and *in vivo* models [18,20,21].

To address the issues described above, we investigated whether THA-coated SLN can retain sufficient complexation with antibacterial ON to form stable lipid-based complexes and whether it is possible to optimize the ratio of THA/ON whilst retaining biological activity. We studied Transcription Factor Decoys (TFD) as antibacterial ON: they are short double stranded DNA molecules that act on novel genomic targets by capturing key regulatory proteins to block essential bacterial genes and defeat infection [22]. In this study two different TFD were used: SigH, which specifically blocks the key *sigma* factor of transition phase in *C. difficile*, and the Ferric Uptake Regulator (Fur), which controls import of the essential micronutrient iron into *E. coli* under limiting conditions: growth of *E. coli* lacking Fur is normal in iron rich media but is severely inhibited in iron depleted media [23].

2. Material and methods

2.1. Materials

Cholesteryl acetate, cholesteryl palmitate, 2-phenylethanol, polyoxyethylene (40) stearate, protamine sulfate salt from Herring (Grade III), heparin sodium salt and phosphate buffered saline (PBS, pH 7.4) were purchased from Sigma-Aldrich (Italy), while cholesteryl butyrate was from TCI Chemicals Europe (Belgium). Epikuron®200 (92% phosphatidylcholine) (PC) (Cargill, Italy) was supplied by ACEF (Italy), which was also the supplier for ascorbyl palmitate and butyl alcohol, while sodium taurocholate was acquired from PCA (Italy). Fluorescent probes DiO (3,3-dioctadecyloxacarbocyanine), DiD (1,1′-dioctadecyl-3,3,3′,3′tetramethylindodicarbocyanine), and DiI (1,1′-dioctadecyl-3,3,3′,3′-tetramethylindocarbocyanine) (Biotium, USA) were purchased from VWR (Italy), as well nucleic acid gel stain Gel Red® (Biotium, US). Dynasan® 116 was kindly given by Cremer Oleo Division (Germany). Sepharose CL-4B was purchased from Sigma-Aldrich (Italy). The 12-bis-THA (THA) was synthesized by Shanghai Chempartner Co. Ltd. Reagents used for gel electrophoresis were purchased from several suppliers, agarose DNA grade from VWR (Italy), TBE 10X from Amresco (USA), and Xylene Cyanol and Bromophenol Blue from Merck (Italy). All organic solvents, HPLC grade, were purchased from Merck (Italy).

Bacterial growth media, culture plasticware, poly-lysine coated microscopy glass slides, and Fluoroshield® mounting media were obtained from Sigma Aldrich (UK); the McFarland turbidity standard and the wheat germ agglutinin lectin conjugated with tetra-methyl rhodamine or with AlexaFluor® 647 were purchased from ThermoFisher (UK).

All TFD were manufactured and purified by HPLC at AxoLabs (Kulmbach, Germany). The SigH dumbbell TFD (SigH DB TFD), used mainly for SLN development and characterization, consists of 77 bp, whereas the Ferric Uptake Regulator hairpin TFD (Fur HP TFD), which was selected for efficacy proof of concept in *E.coli*, comprises 59 bases (See supplementary material for complete sequences). AlexaFluor® 488 fluorescent dye ($\lambda_{ex/em}$ = 495/519 nm) was attached to the 5′ end for fluorescent labelling (AF488 Fur HP TFD), needed to study interactions between TFD-SLN complexes and bacteria by fluorescence microscopy.

All oligonucleotides were resuspended in distilled, nuclease-free water at concentration of 0.5 μM, annealed by heating at 95 °C for 2 min and allowed to cool to room temperature for 15 min. They were then purified by ethanol precipitation, resuspended again in distilled RNase-free water and stored at -20 °C until use.

2.2. SLN preparation

2.2.1. Anionic SLN

Anionic SLN were prepared by oil-in-water (O/W) warm microemulsion method reported elsewhere [24,25]. Briefly, the selected lipid matrix was heated above its melting point, then it was mixed under magnetic stirring with an aqueous phase at the same temperature containing surfactants (phosphatidylcholine and polyoxyethylene (40) stearate) and co-surfactants (sodium taurocholate, butyl alcohol and 2-phenyl ethanol) in an appropriate mixture to stabilize O/W interface and promote spontaneous microemulsion formation. The microemulsion was immediately dispersed into water at 2–3 °C (ratio 1:10 v/v) under mechanical stirring (1900 rpm). Three anionic SLN prototypes were obtained depending on matrix composition: A-Chol (cholesteryl esters mixture), A-TP (tripalmitin) and A-TPAP (tripalmitin and ascorbyl palmitate mixture). Obtained SLN dispersions were then washed (6X) by tangential flow filtration (TFF) (Vivaflow 50, RC membrane, 100 KDa MWCO, Sartorius Stedim Biotech GmbH, Italy) for purification, all components were finally reduced to regulatory acceptable concentrations [26].

2.2.2. TFD-THA-SLN complexes preparation

12-bis-THA (THA) and TFD (oligonucleotides, ON) were added to preformed SLN by a coating technique, exploiting electrostatic interaction. Briefly, THA saturated aqueous solution (800 μg/mL) was added drop by drop into anionic SLN dispersions under magnetic stirring, in a ratio 1:1.5 (v/v). After 15 min of incubation, obtained dispersion was washed (3×) by tangential flow filtration membrane in order to remove free THA. Filterability of THA through used membrane was previously assessed to ensure effectiveness of this washing process.

Cationic THA-coated SLN (C-Chol and C-TP SLN respectively) were then incubated in orbital shaker (400 rpm, 30 min) with TFD aqueous solution to achieve different TFD final concentrations (10–160 μg/mL) obtaining cationic THA-SLN complexed with oligonucleotides: ON-C-Chol and ON-C-TP SLN.

In order to ameliorate TFD interaction with the carriers, other formulations were prepared with a second layer of THA onto previous TFD layer (C-ON-C-Chol and C-ON-C-TP respectively), by simple addition of a small volume (100 μL) of THA aqueous solutions at different concentrations (100–320 μg/mL) to ON-C-Chol and ON-C-TP prototypes. Final washing was carried out by tangential flow filtration, as previously described.

Finally, as a control, a different type of cationic SLN (C-TPAP SLN) were prepared by substituting THA with the cationic polypeptide protamine as SLN coating. Similarly, protamine aqueous solution (2 mg/mL) was added dropwise onto anionic SLN dispersion (A-TPAP) under magnetic stirring, in a 1:5 (v/v) ratio. Tangential flow filtration (3×)

Table 1
SLN prototypes composition and codification according to layers composition.

Lipid Matrix	Type of SLN and layers composition						
	Anionic	Addition of cationic compound 1st layer	Cationic, single layer	TFD addition	Cationic, single layer, TFD loaded	Addition of cationic compound 2nd layer	Cationic, double layer, TFD loaded
Cholesteryl esters mixture	A-Chol	→ + *THA*	C-Chol	→ + *TFD*	ON-C-Chol	→ + *THA*	C-ON-C-Chol
Tripalmitin	A-TP	→ + *THA*	C-TP	→ + *TFD*	ON-C-TP	→ + *THA*	C-ON-C-TP
Tripalmitin and Ascorbyl palmitate	A-TPAP	→ + *PROT*	C-TPAP	→ + *TFD*	ON-C-TPAP	–	–

THA: 12-bis-THA-Cl; PROT: Protamine.

was performed after 15 min of incubation to remove free protamine. Finally, cationic protamine-SLN were incubated with TFD aqueous solutions in order to achieve different TFD final concentrations (10–160 μg/mL) (ON-C-TPAP). Table 1 summarizes SLN codification according to layers and composition. Fluorescent SLN for further SLN characterization and for uptake studies by confocal microscopy were prepared by adding hydrophobic fluorophores DiO, DiI or DiD to the oily phase of microemulsion, at molar percentage of PC (2%).

2.3. SLN characterization

Several techniques were used to characterize obtained SLN.

2.3.1. Determination of particle size and surface charge

Average dimensions of SLN were evaluated by Dynamic Light Scattering (DLS), while Zeta potential was measured by laser Doppler velocimetry (LDV). For size measurement SLN dispersions were diluted (1:100) in bidistilled water, whereas for zeta potential measurement samples were diluted (1:20 or 1:50) in 1 mM NaCl. All measurements were performed in triplicate on a Malvern Zetasizer-Nano ZS (UK) , at 25 °C.

2.3.2. Chemical composition

Chemical composition of carriers was assessed by HPLC-UV analysis: THA and protamine content was considered for determination of surface coating efficiency, whereas phosphatidylcholine (PC) content was used to check final composition of SLN (i.e. after washing steps) and chemical stability over time. HPLC samples were prepared as follows: SLN were disrupted by dilution first with tetrahydrofuran and then with corresponding HPLC eluent (See supplementary material for chromatographic methods).

To establish the best conditions for electrostatic interaction between THA and SLN, several dilutions of SLN dispersions were incubated with different amounts of THA and samples were then purified as previously described: the molar ratio among PC and THA in purified sample was determined by HPLC-UV analysis.

2.3.3. Morphological analysis

Morphological characterization was performed by Field Emission Scanning Electron Microscopy (FESEM) (ZEISS Supra 40, DISAT, Polytechnic of Turin, Italy). SLN dispersions were diluted in a range 1:500 to 1:5000 in bidistilled water, then 4 μL were poured on a silica platelet and dried under light vacuum. Samples were observed at tension values ranging from 1 to 5 kV.

2.3.4. DNA binding capacity

The ability of cationic SLN to bind TFD was evaluated by gel retardation assay using agarose gel electrophoresis (See Methods in supplementary material for specific conditions). Evaluated samples were: TFD-SLN complexes, their corresponding samples after TFD extraction, and free TFD as control. For TFD extraction, SLN were disrupted by dilution with isopropanol and TFD was then precipitated by centrifugation (10,000 rpm, 10 min, 4 °C). Two further washing steps with methanol were performed in order to solubilize THA and to release the TFD, followed by a centrifugation step, as previously described. Finally, precipitated DNA was resuspended in bidistilled sterile water. For SLN containing protamine, TFD was released by incubation with heparin solution (5 mg/mL) in a ratio 25:1 (w/w) with DNA, conditions in which heparin binds to the cationic polymer, thus releasing the DNA [27].

2.4. Deoxyribonuclease I (DNase I) protection assay

The protection of TFD against DNase I enzymatic activity was tested in reaction buffer rich in Mg^{2+} and Ca^{2+}, as those cations are essential for DNase I activity.

TFD-SLN complexes dispersions were diluted in reaction buffer containing DNase I (1:4), samples were then incubated at 37 °C for 30 min in an orbital shaker (350 rpm), and finally a volume of EDTA solution was added to stop the enzymatic activity by chelation of essential cations (Mg^{2+} and Ca^{2+}). TFD was extracted from the complex and precipitated as described above. Samples were analyzed by agarose gel electrophoresis, as previously reported, to evaluate TFD integrity. First, increasing amounts of DNase I (0.01–1 U DNase I/μg TFD) were tested to find the adequate concentration needed to degrade a fixed amount of free TFD. Two types of controls were prepared with same amount of free TFD: negative control (non-degraded TFD), in which the stop solution was added at the beginning of the experiment, and a positive control, where TFD was fully degraded. The integrity of TFD-SLN complexes was evaluated by comparing with both controls.

2.5. SLN interaction with bacteria

To evaluate SLN ability to deliver TFD into bacteria, their interactions was studied by confocal microscopy and flow cytometry. Selected SLN formulations with favourable stability and TFD protection were used for these studies and, in particular, SLN with two layers of THA and SLN with one layer of protamine, all of them at TFD concentration of 40 μg/mL (C-ON-C-Chol, C-ON-C-TP and ON-C-TPAP). Interactions were studied after 1 h and 4 h of incubation.

2.5.1. Confocal microscopy

For qualitative interaction studies by confocal microscopy, all tested SLN were labelled with the Infra-Red dye, DiD ($\lambda_{ex/em}$ = 644/663). Fluorescently labeled TFD (AF488 TFD) were used to prepare the complexes with SLN. Moreover, two control samples were included in the analysis: (i) free TFD in water (40 μg/mL), and (ii) THA-TFD self-assembling nanoparticles, prepared and fully characterised as described by Marin-Menendez et al. [12]. Bacteria were stained with a wheat germ agglutinin lectin conjugated with tetra-methyl rhodamine (TMR WGA) fluorescent membrane dye ($\lambda_{ex/em}$ = 555/580).

E.coli strain DH5α was grown in LB broth until reaching an optical density (OD) of 0.3 (630 nm), as described in the supplementary material (Supplementary Methods). This fresh culture was then incubated with SLN suspension (1:1 v/v) under gentle shaking at room temperature and in the dark for 1–4 h. TMR-WGA dye (10 μg/mL) was added to

the samples during the last 30 min of incubation in order to stain bacteria membranes.

The samples were then spotted onto poly-lysine coated microscopy glass slides and left to adhere for 1 h in a humid chamber in the dark. Glass slides were gently washed three times with sterile PBS, dried and mounted with Fluoroshield® mounting media before they were covered with cover slips; they were then left 15 min for settling at room temperature in the dark and stored at 4 °C overnight. Next day, the slides were analyzed by Leica SP5 confocal microscope using a 63× objective. The images obtained were processed with Image-J software (NIH Image).

2.5.2. Flow cytometry

Bacterial interaction with selected SLN formulations was also evaluated by flow cytometry.

Bacteria cultures were incubated with SLN as described for confocal microscopy above. At the end of incubation, bacterial suspensions were pelleted (5 min, 4000*g*) and resuspended in an equal volume of PBS. Samples were then diluted in PBS (1:40) and measured with a FC500 flow cytometer (Beckman Coulter).

The protocol for bacteria detection through flow cytometry was first optimized as fully described in Supplementary material (Table S1, Figs. S6-S10). Briefly, the scatterplots (forward scatter, side scatter and fluorescence intensity) of unlabelled control bacteria were evaluated first. Then, bacteria were labelled with a WGA-AlexaFluor® 647 ($\lambda_{ex/em}$ = 650/665, Life Technologies, UK) membrane dye to confirm the proper gating strategy and analyzed using FL4 laser (635 nm). Cells were then incubated with non-labeled SLN and the gates on the Forward Versus Side Scatter dot plots were once again adjusted to be sure to select only the bacterial cell population and eliminate debris due to residual SLN in solution.

To quantify the signal of delivered TFD, C-ON-C-TP and ON-C-TPAP were loaded with fluorescent AF488 TFD, as for confocal microscopy analysis. In parallel, and in order to quantify the signal of SLN interacting with bacteria, the lipid matrix was labelled with DiD.

Single cells were gated using the FS vs SS scatterplots, previously optimized with non fluorescent SLN, and histogram on the corresponding Fluorescence channels (488 nm excitation FL1 laser for TFD and 635 nm excitation FL4 laser for DiD) were used to evaluate the percentage of bacteria that were positive to TFD and to SLN signals respectively. Only the cells that were over the threshold set with control samples were considered . The two analyses were performed separately in order to avoid problems of compensation among the two different fluorochromes. At least 10,000 events were analyzed per condition. Results were analyzed with Kaluza software (Beckman Coulter, UK).

2.6. Antibacterial activity

2.6.1. Minimum inhibitory concentration (MIC) test

Antibacterial activity of SLN was measured on *Escherichia coli* K12 strain (DH5α) using the minimum inhibitory concentration (MIC) assay. The standard broth microdilution method was in line with current Clinical and Laboratory Standards Institute (CLSI, USA) approved methodologies [28] and with the protocols previously described [29,30]. Briefly, serial dilutions of Fur HP TFD-loaded SLN were incubated with a single clone of bacteria previously grown overnight on a fresh culture plate in an orbital shaker at 37 °C for 14–18 h. The final range of tested SLN concentrations was from 1300 μg/mL to 0.65 μg/mL of PC (corresponding to THA concentration of 11 μg/mL and 5.5 ng/mL in THA coated SLN). At the end of incubation, plates were evaluated visually and by reading the optical density (OD) at λ = 630 nm with a plate reader (POLARstar Omega, BMG Labtech GmbH). MIC was considered as the concentration at which the OD was observed not to increase due to antibacterial activity of SLN. Each experiment was performed in triplicate.

2.6.2. MIC in iron-limited media

The *E. coli* K-12 MG1655 strain was grown at 37 °C in MOPS minimal media supplemented with 0.2% glucose (GMM) and 2 mM sodium nitrate. The media was stored under microaerobic conditions for 24 h prior to use. Under these conditions MIC was determined by adding a range of concentrations of SLN to broth inoculated with MG1655, 1 x10^6 colony-forming units (CFU) per mL. The final range of tested SLN concentrations was from 1000 μg/mL to 0.98 μg/mL of PC. These were cultured for 16 h under microanaerobic conditions before the concentration of bacteria (CFU/mL) was determined by plating of serial dilutions on LB agar plates and counting of subsequent bacterial colonies. Each experiment was repeated in triplicate.

2.7. In vitro and in vivo cytotoxicity studies

2.7.1. Cytotoxicity MTT assay

Caco-2 (colorectalcolon adenocarcinoma cells, ATCC HTB-37) and Calu-3 (human epithelial lung adenocarcinoma cells, ATCC HTB-55) were cultured at 37 °C in Dulbecco's Modified Essential Medium (DMEM) supplemented with 10% heat-inactivated fetal bovine serum (FBS) and 2% penicillin–streptomycin. Cells were seeded in 96-well plates at 5 × 10^4 cells/cm^2, left to grow until 70–80% confluency and then culture media was removed and cells were incubated with 100 μL of serum-free media containing serial dilutions of the tested SLN formulations. Cells were incubated with the SLN for 24 h and 48 h, then culture media was removed and MTT assay was performed . Briefly, cells were incubated with an MTT solution (400 μg/mL of MTT in media) for 2 h at 37 °C. The MTT solution was then removed and 200 μL of DMSO was added and the absorbance of the plates was read at 570 nm using a Luminometer (Glomax Explorer, Promega). Each experiment was performed three times; acetaminophen was used as a positive control of cytotoxicity.

2.7.2. In vivo toxicity studies in Xenopus laevis embryo model

All experiments were performed in compliance with the relevant laws and institutional guidelines at the University of East Anglia. The research has been approved by the local ethical review committee according to UK Home Office regulations. *Xenopus laevis* embryos were obtained as previously described [31]. Embryos were grown at 23 °C until they reached stage 38, and then plated in 48-well plates (5 embryos/well, n = 15 used for each condition) in 0.1× MMR media containing the serial dilutions of SLN at 6 different PC concentrations (from 1.5 mg/mL to 46.8 mg/mL) and incubated at 18 °C. Non-treated embryos were used as control. The mortality and the morphological changes of the embryos were recorded every 24 h until embryos reached stage 45. The experiment was repeated twice.

2.8. Statistical analysis

Statistical analysis was performed using GraphPad Prism Software v7.04.

3. Results and discussion

3.1. SLN preparation and characterization

Different SLN were successfully obtained by warm microemulsion method with different lipid matrices and combinations of surfactants and co-surfactants. These SLN were then used as a scaffold for their further coating with THA and TFD. As shown in Table 2, the particles presented a size around 100 nm and displayed negative zeta potential. Incorporation of ascorbyl palmitate (A-TPAP) made the particles slightly bigger but with a lower negative zeta potential, an effect that has been previously reported for other lipid nanocarriers containing ascorbyl palmitate [32,33]. Coating with THA did not affect size, but caused inversion of zeta potential from negative to positive, due to

Table 2
Physicochemical characterization of SLN: size (nm), PdI and Zeta potential (mV) determined by DLS (Values are mean ± SD (n = 3–20)).

Lipid matrices	SLN ID	Layers composition			SLN physicochemical properties		
		THA	Protamine	TFD	Size (nm)	PdI	Z potential (mV)
Cholesterol ester mixture	A-Chol	–	–	–	90 ± 5	0.224	−19 ± 5
	C-Chol	Y	–	–	91 ± 6	0.235	+16 ± 2
	ON-C-Chol	Y	–	Y	91 ± 2	0.249	+14 ± 3
Tripalmitin	A-TP	–	–	–	101 ± 10	0.265	−21 ± 5
	C-TP	Y	–	–	93 ± 10	0.267	+14 ± 3
	ON-C-TP	Y	–	Y	90 ± 3	0.285	+12 ± 2
Tripalmitin + ascorbyl palmitate	A-TPAP	–	–	–	119 ± 12	0.282	−28 ± 3
	C-TPAP	–	Y	–	124 ± 14	0.272	+12 ± 1
	ON-C-TPAP	–	Y	Y	110 ± 11	0.280	+10 ± 3

Y: component present. SigH DB TFD concentration used was 10 μg/mL.

effective interaction between the cationic compound and SLN surface. Coating with protamine showed similar behavior.

THA coating efficiency was very high, with a value of association to SLN equal to 88% ± 5% for C-Chol and 89% ± 6% for C-TP. Furthermore, recurrent value for molar ratio between PC and THA was found, around 3.6% ± 0.3% (n = 5) for all different THA concentrations tested, suggesting saturable loading of THA into the SLN matrix surface. This trend was found for both SLN compositions and it was taken as reference value in optimization of layering process, purification and scaling studies.

Protamine content was analyzed by HPLC; the interaction of the polypeptide with SLN surface was also high, with 64 ± 4% of the initial protamine detected after TFF washing step, which is in agreement with data reported for other lipid nanocarriers containing PEG stearate [34].

The incubation with TFD (final concentration 10 μg/mL) slightly reduced zeta potential of SLN coated with cationic molecule. The molar ratio between the bolaamphiphile and the oligonucleotide was determined as 964:1 for ON-C-Chol and 988:1 for ON-C-TP, which implies a positive-to-negative charge ratio $Z_{+/-}=13$. In the case of protamine-coated SLN, the molar ratio between the polypeptide and TFD was 112:1, which leads a positive-to-negative charge ratio $Z_{+/-}=14.5$. The absence of complexes between THA or protamine and TFD was confirmed by DLS analysis and gel filtration chromatography. Briefly, fluorescent dye (DiO) was loaded into SLN matrix as a particle marker, and fluorescent TFD-loaded SLN were loaded into Sepharose CL-4B column (28 cm), then fractions of 1 mL were collected from the column over time. Analysis of the eluted fractions showed the presence of TFD only in the fractions where SLN were recovered, confirmed by HPLC determination of SLN components (PC, THA or protamine) and the fluorescent marker DiO by UV–Vis spectrophotometry (data not shown), being a further confirmation of effective complexation between TFD and SLN. Moreover, no complexes between THA/protamine and TFD were detected in any of the eluted fractions.

Images by Field Emission Scanning Electron Microscopy (FESEM) showed that SLN displayed a round shape and indicated the presence of populations of different size, which would be in agreement with the polydispersity indices (0.2 < PdI < 0.26) obtained by DLS analysis. Representative images of anionic SLN A-Chol and A-TP, as well final formulation C-ON-C-Chol and C-ON-C-TP that will be decribed later have been obtained (Fig. 1).

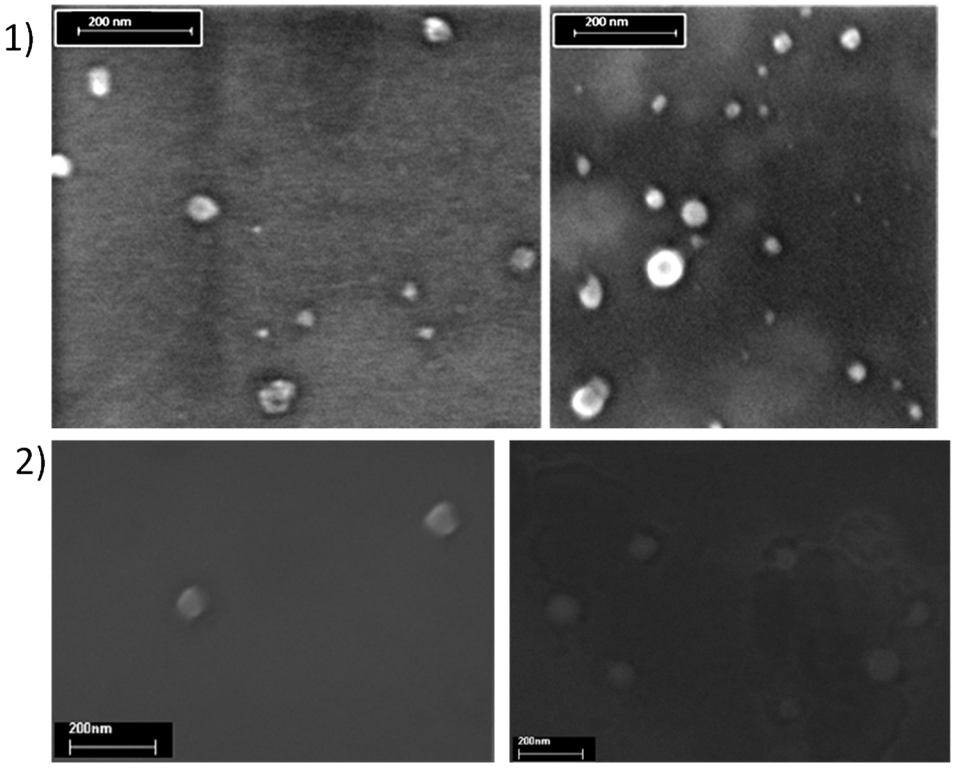

Fig. 1. Field Emission Scanning Electron Microscopy (FESEM) images: (1) Anionic SLN prepared with a mixture of cholesteryl ester (A-Chol, top left image) or with tripalmitin (A-TP, top right image); (2) final cationic SLN containing TFD and double layer of THA with a mixture of cholesteryl ester (C-ON-C-Chol, bottom left image) or with tripalmitin (C-ON-C-TP, bottom right image) Images were captured at 1–5 kV.

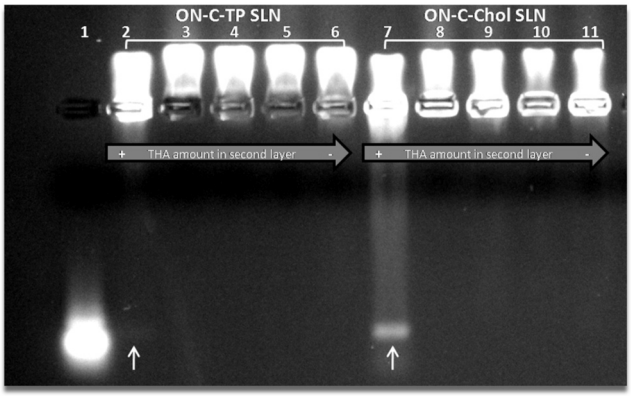

Fig. 2. Agarose gel electrophoresis of SLN having decreasing amount of THA for second layer coating. Lane 1 correspond to free TFD control (10 μg/mL); Lanes 2 and 7 correspond to ON-C-TP and ON-C-Chol respectively; Lanes 3–6 and 8–11 correspond to SLN with the second coating of THA in concentrations ranging from 320 to 100 μg/mL. Arrows indicate lanes in which free TFD band was observed.

3.2. DNA binding capacity of THA-SLN cationic complexes

The visualization of agarose gel after electrophoresis showed ON-C-TPAP were able to effectively bind all the added TFD (10 μg/mL), whereas for ON-C-Chol and ON-C-TP SLN a band of free TFD appeared, much more evident in ON-C-Chol (Fig. 2). In order to reduce free TFD, a small amount of THA was added over TFD layer, forming further external THA coating.

As expected, the addition of a further THA layer is an efficient way to increase TFD binding capacity, with no band of free TFD at all concentrations tested (100–320 μg/mL THA) (Fig. 2). The lowest concentration of THA in the second layer was selected for biological studies because of safety considerations.

As shown in Table 3, SLN with double THA layers displayed no changes in size and PdI and only a slight increase in positive zeta potential was observed (from + 16 mV to + 18 mV in C-ON-C-Chol and from + 14 mV to + 18 mV in C-ON-C-TP). The total amount of THA in the final SLN was comparable in both SLN types, with the ratio between THA and PC raised up to 5% ± 1% (n = 6) in both cases. The molar ratio between the bolaamphiphile and the oligonucleotide was raised to 1073:1 for C-ON-C-Chol and 1052:1 for C-ON-C-TP, which gives a positive-to-negative charge ratio $Z_{\pm}$ = 14, comparable to value found for protamine-coated SLN.

Furthermore, to determine the maximum amount of TFD that could be attached to SLN surface, ON-C-Chol and ON-C-TP were successfully prepared with increasing amounts of TFD, starting from concentration 10 μg/mL and increasing 16-fold. Then, a second coating with THA was applied to TFD layer. Increasing TFD amount did not change the SLN size and PdI at any concentrations tested, whereas Z potential decreased as TFD content increased, reaching values close to neutrality (Chol matrix) or even negative (TP matrix) for the highest concentration tested. The second layer of THA did not affect particle size, zeta potential was positive with very similar values in all cases (See supplementary material, Fig. S1).

Agarose gel electrophoresis (Fig. 3) showed both kinds of SLN were able to bind up to 5 times more TFD by increasing it concentration, and no TFD free band was seen after the addition of THA second layer. A further increase in TFD concentration showed a band of free TFD. This free TFD was again more evident in ON-C-Chol SLN type. Formulations showing more free-TFD displayed lower values of positive zeta potential, which could indicate only partial coating of underlying TFD layer. Finally, samples containing 40 μg/mL of TFD were selected for further studies. In this case molar ratio between THA and TFD was reduced to 266:1 for both SLN types (Chol and TP), which reaches $Z_{\pm}$ = 3.5.

For comparative purpose, ON-C-TPAP (protamine) was evaluated for its ability to bind higher amounts of TFD. The behavior was the same as for the other two prototypes, with reduction of positive zeta potential at increasing amount of TFD, without significant changes in size. The agarose gel after electrophoresis did not show free TFD band in the range of tested concentrations (10–40 μg/mL TFD). For ON-C-TPAP containing 40 μg/mL of TFD, the molar ratio between protamine and ON was 28:1, with $Z_{\pm}$ = 3.6. These data confirm that final positive-to-negative ratio was comparable for all three TFD-SLN complexes prepared, although differences in composition and in cationic moieties used for coating.

3.3. Dnase I protection studies

A crucial characteristic of DNA carriers is their ability to protect DNA from enzymatic degradation by DNase, improving chances of cellular internalization and maintaining transfection efficacy [35,36]. The amount of DNase I needed to degrade free TFD in appropriate experimental timescales was first assessed by screening enzyme masses ranging from 0.01 to 1U DNase I per 1 μg of TFD. Agarose gels electrophoresis of these samples showed that 0.2 U DNase I per μg of TFD produced a partial degradation in 30 min, and gradual increase in concentrations led to full digestion of nucleic acids (data not shown). 0.6 U DNase I per μg of TFD was finally selected as the optimal enzyme amount to ensure total degradation of free TFD. Unbound TFD was degraded by the enzyme into smaller fragments that ran farther in the gel compared to intact TFD (Fig. 4, lanes A1 and B1, negative controls) that also showed reduced fluorescent band intensity (Fig. 4 lanes A2, A7, and B2, positive controls). For ON-C-Chol (Fig. 4A), absence of THA second layer led to TFD degradation (Fig. 4A lane 4 compared to 3, non-treated SLN), while particles with external THA layers (C-ON-C-Chol) were able to protect TFD at both concentrations tested, 10 and 40 μg/mL. No difference in band intensity was observed between non-treated and treated samples after the effective extraction of TFD from the

Table 3
Physico-chemical characteristics of SLN before and after second coating with THA (100 μg/mL): size (nm), PDI and Zeta potential (mV) determined by DLS; THA and PC final concentration determined by HPLC (Values are mean ± SD (n = 7)).

SLN	Layers Composition			Physical and Chemical Properties				
				DLS			HPLC (UV–vis)	
	THA 1st layer	TFD	THA 2nd layer	Size (nm)	PdI	Z Pot (mV)	THA (μM)	PC (mM)
C-Chol	Y	–	–	91 ± 6	0.235	+16 ± 2	405 ± 2	11.3 ± 0.9
ON-C-Chol	Y	Y	–	91 ± 2	0.249	+14 ± 3	nd	nd
C-ON-C-Chol	Y	Y	Y	97 ± 7	0.227	+18 ± 1	451 ± 2	9.5 ± 0.9
C-TP	Y	–	–	93 ± 10	0.267	+14 ± 3	415 ± 2	11.3 ± 1.2
ON-C-TP	Y	Y	–	90 ± 3	0.285	+12 ± 2	nd	nd
C-ON-C-TP	Y	Y	Y	92 ± 7	0.268	+18 ± 1	442 ± 3	8.8 ± 0.9

Y: component present. SigH DB TFD concentration used was 10 μg/mL.

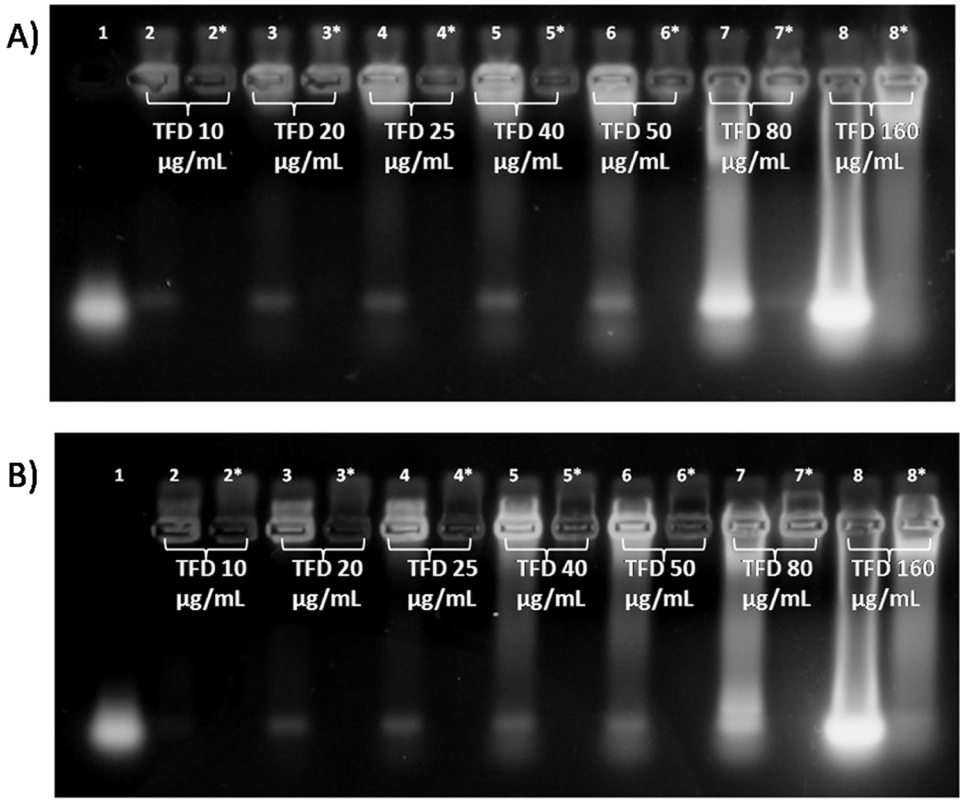

Fig. 3. Agarose gel electrophoresis of cationic THA-SLN incubated with increasing amount of TFD: (4A) ON-C-Chol, (4B) ON-C-TP. Lane 1 correspond to free TFD control (10 µg/mL) *THA second coating added.

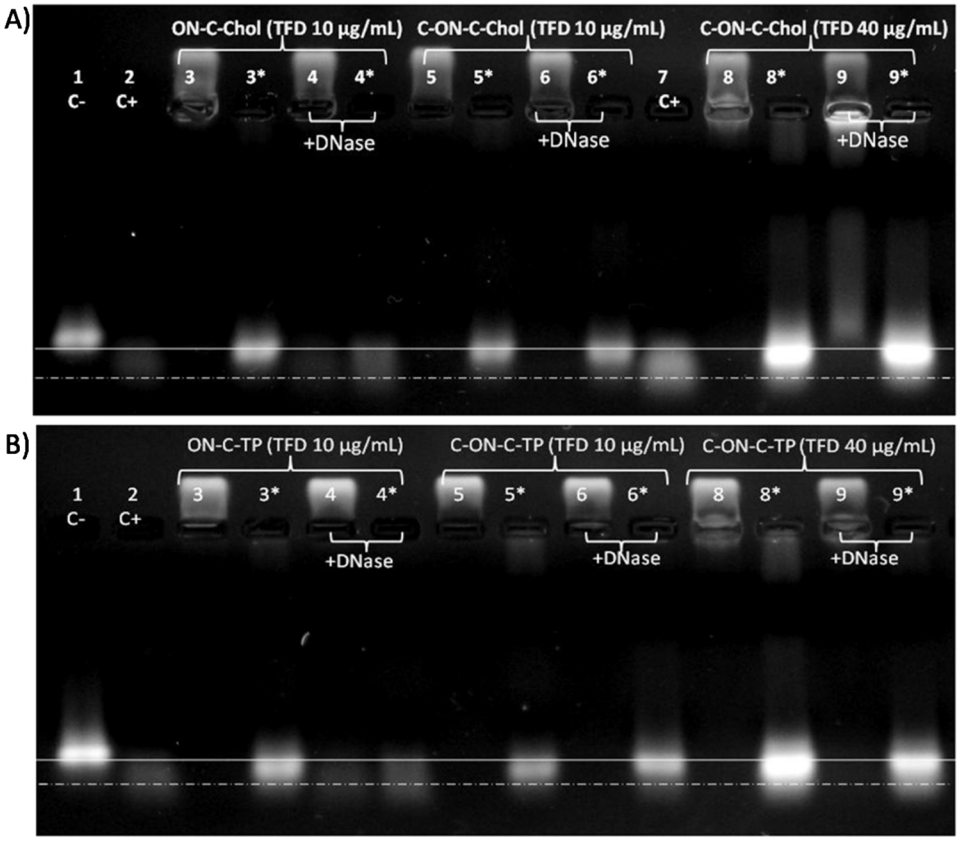

Fig. 4. DNase I protection assay. Agarose gel electrophoresis: Lanes A1 and B1 correspond to negative control, whereas lanes A2, A7 and B2 correspond to positive control. (A) ON-C-Chol and C-ON-C-Chol, (B) ON-C-TP and C-ON-C-TP (*indicates run of TFD extracted from the corresponding sample). Continuous line indicates intact DNA, dots line indicates degraded DNA.

complexes (Fig. 4A lane 6 compared to lane 5 for 10 μg/mL; lane 9 compared to lane 8 for 40 μg/mL). The same behavior was observed for ON-C-TP (Fig. 4B): absence of an external THA layer caused greater TFD degradation (Fig. 4B lane 4 vs lane 3), whereas THA second layer preserved TFD after incubation with DNase I at both tested concentrations (Fig. 4B lane 6 vs lane 5 and lane 9 vs lane 8).

These results suggest that external THA generates full TFD protection against enzymatic degradation, probably because of increased masking and condensed state of TFD, a structural conformation which may help in making it refractory to DNase I. These observations are consistent with published circular dichroism spectroscopy data demonstrating DNA condensation by 12-bis-THA [37,38].

Enzymatic degradation assays carried out on ON-C-TPAP at highest concentration (40 μg/mL TFD) also showed TFD was fully protected from enzyme (See supplementary material, Fig. S2), in agreement with data previously reported for other gene carriers based on protamine [39–41].

3.4. SLN interaction with bacteria

3.4.1. Confocal microscopy

Confocal microscopy analysis of SLN-bacterial interactions was permitted by successful SLN labeling with DiD. Dye entrapment efficiency was very high (> 95%), and labeling proved to be stable after washing 6x with TFF (data not shown). Before incubation with bacteria C-ON-C-Chol, C-ON-C-TP and ON-C-TPAP were complexed with 40 μg/mL of fluorescent Fur HP AF488TFD (AF488-TFD) and validated by DNase I protection assay (data not shown), as previously reported for non-fluorescent TFD. Neither the different TFD nor the addition of the fluorescent dye affected overall physicochemicals characteristics of SLN.

Representative images of SLN interaction with bacteria were obtained after 1 and 4 h of incubation (Figs. 5 and S3). Bacteria, here labeled with the red WGA membrane lectin dye, can be seen adhered to the glass slides. As expected, the extent of interaction between bacteria and anionic SLN (A-Chol, A-TP and A-TPAP) was quite low up to 4 h. This was most likely due to repulsive forces between the negatively charged SLN and the bacterial membranes (Fig. 5A, A′ D, D′, G and G′).

In contrast, cationic SLN displayed rapid and extensive interaction with bacterial cells, independent of their lipid composition. This was observed for THA-coated C-Chol and THA-coated C-TP as well as for protamine-coated C-TPAP: all displayed extensive membrane binding and cellular aggregation especially after 4 h incubation (Fig. 5 B′, E′ and H′). For all the different samples the signal of DiD (lipid matrix labelling) was mostly observed interacting with the external surface of the bacteria and very low intracellular particle delivery could be observed at both time points (1 and 4 h). This can be appreciated even better in Fig. S3 which reports the three fluorescence channels separated.

Although the lipid core did not influence the SLN-bacteria interaction, it seemed to have an important role in determining the TFD intracellular delivery. Specifically, when incubating bacteria with the cholesteryl ester based C-ON-C-Chol, most of the SLN and TFD signal is observed around the membrane without penetrating into the cytoplasm (blue and green signal in Fig. 5C and C′). Here, a high colocalization between membrane, SLN and TFD dyes was observed at both time points of analysis (yellow signal in Fig. 5C and C′). Interestingly, more extensive TFD intracellular signal was observed with tripalmitin based C-ON-C-TP and ON-C-TPAP. For C-ON-C-TP SLN, a strong membrane affinity was still observed for the first time point of analysis (Figs. 5F and S3D–F), whereas after four hours of incubation, the intracellular signal seems higher and in some cases the oligonucleotide signal was observed diffused in the bacterial cytoplasm (Fig. 5F′ and I′, *S3* D′-F′ and G′-I′). This was observed since the first time point (Fig. 5I) in the case of ON-C-TPAP. In these cases, a low colocalization was observed between TFD and SLN signals, suggesting that the SLN-TFD complex is disrupted during TFD uptake.

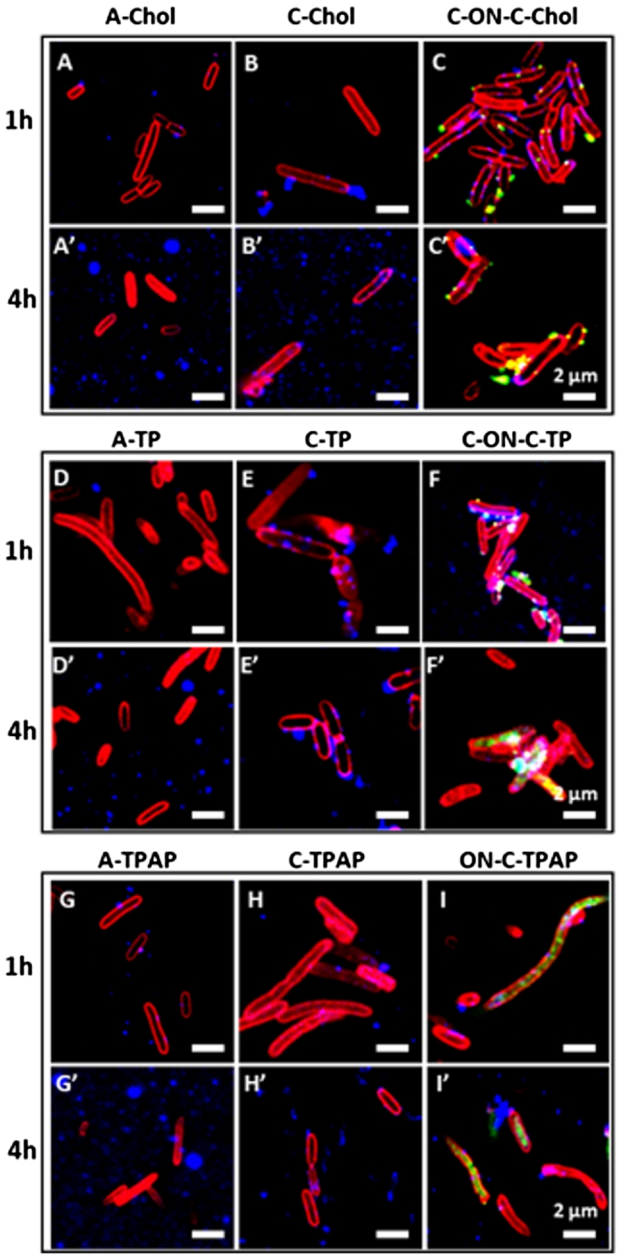

Fig. 5. Confocal microscopy images. Interaction between E.coli DH5α bacteria and different types of SLN after 1 h and 4 h of incubation. Bacteria membranes are visualized in red, DiD labelled SLN in blue and Fur HP AF488 TFD in green. (Scale bar = 2 μm). (For interpretation of the references to colour in this figure legend, the reader is referred to the web version of this article.)

3.4.2. Flow cytometry

Semi-quantitative data of SLN interaction with bacteria were obtained by flow cytometry. Only tripalmitin-based SLN were used for these experiments, as they represented the most promising agent in terms of intracellular TFD delivery by confocal microscopy. As fully described in supplementary material, acquisition parameters were optimized on control cells and SLN alone to allow specific identification of the bacteria population and to quantify the interaction between bacteria and the delivery system.

To evaluate TFD delivery by flow cytometry, SLN were prepared with fluorescently labelled AF488-oligonucleotides and incubated with cells for 1 and 4 h. In a separate set of experiments, the lipid matrix was labelled with DiD and the SLN-bacteria interaction was measured, in order to avoid problems related to non-specific fluorescence detection

Table 4
Quantitative evaluation of SLN interaction with bacteria after 1 h and 4 h of incubation: percentage of bacteria positive to the TFD, labelled with AF488, and positive to SLN, labelled with DiD.

Samples	TFD (AF488, %)		SLN (DiD, %)	
	1 h	4 h	1 h	4 h
Control	0.42	0.12	0.1	0.81
A-TP	0.01	0.01	1.13	2.8
C-ON-C-TP	12.5	21.69	65.06	69.69
A-TPAP	0.31	0.43	1.6	4.02
ON-C-TPAP	30.36	31.16	68.86	73.5

between the different channels. In agreement with confocal microscopy data analysis, flow cytometry confirmed that interaction with anionic SLN is very low at both time points, with less than 5% of gated events interacting with DiD labelled SLN even after 4 h of incubation (FL4 laser, 635 nm excitation) (Table 4). This underlines the importance of the positive charge in triggering SLN uptake. After bacteria incubation with cationic SLN (C-ON-C-TP and ON-C-TPAP), a rapid increase in the proportion of positive gated cells was observed. The percentage of stained bacteria for C-ON-C-TP was 65% after 1 h of incubation and almost 70% after 4 h. The percentages were slightly higher for ON-C-TPAP, with 69% and 73.5% of stained bacteria after 1 h and 4 h of incubation respectively.

Results were different when measuring the TFD signal on FL1 channel (488 nm excitation), as only 12.5% and 30.4% of cells were above the threshold that was considered as positive to TFD signal after 1 h of incubation with both C-ON-C-TP and ON-C-TPAP. After 4 h of incubation, these percentages increased up to 21.7% in the case of C-ON-C-TP whereas remained almost unaltered for ON-C-TPAP (31.2%). The increase observed for C-ON-C-TP might suggest that fluorescence of TFD was somehow quenched at early time points, when it was observed that TFD are still interacting with bacteria membranes. After 4 h of incubation, the intracellular diffusion of the TFD, which was observed by confocal microscopy, might lead to dequenching of the TFD signal and a consequent higher percentage of stained bacteria. This was also tested by measuring the fluorescence of SLN in a liquid suspension (Fig. S5). Here it was shown that, when interacting with THA, TFD fluorescence is quenched. Only when THA-TFD interaction is disrupted the fluorescence is fully recovered. The same could happen in cells, where only the SLN outer layer of THA is removed or somehow sequestered by the cells, then TFD is released and fluorescence is dequenched.

On the other hand, confocal microscopy analysis showed that the release of TFD when incubating bacteria with ON-C-TPAP seemed faster, thus limiting the quenching effect described for C-ON-C-TP. This might explain the higher percentage of TFD positive cells measured by flow cytometry after 1 h of incubation, which is almost the same after longer incubation times. Methodological differences and sample sizes in respective methods nonetheless precludes direct comparison between confocal microscopy and flow cytometry analyses. Techniques that permit semi-quantitative evaluations of nanoparticles-cell interactions at a subcellular level are now developing rapidly [42–45], however the present work focussed on the application of confocal microscopy analysis for qualitative study of SLN-bacteria interaction and subsequent intracellular TFD release. Flow cytometry analysis complemented confocal microscopy data with a semi-quantitative evaluation of the SLN-bacteria interactions, but did not allow us to discriminate if the TFD was intracellularly released or remained interacting with the membrane, as no strategies to distinguish between interacting and internalized SLN were developed in the present study.

Overall, these results confirm that both THA and protamine are cationic agents that lead to a high interaction between SLN and bacteria. Moreover, the intracellular release of TFD, even if it was observed in a reduced number of bacteria, seemed to be improved when tripalmitin was used as lipid core. The exploitation of super-resolution microscopy techniques would further illuminate the entry pathways and mechanics of SLN penetration into bacterial cells.

3.5. Antibacterial activity

The TFD used in this study (Fur HP TFD) targets the Fur transcription factor that controls iron homeostasis in *E. coli* and other bacteria [23]. TFD-mediated inhibition of Fur is expected to deregulate iron-transport mechanisms and curtail response to concomitant oxidative and nitrosative stress, and would be expected to prevent bacterial growth under microaerobic conditions in iron-limited media supplemented with 2 mM nitrate. These conditions mimic those likely to be found in infected parts of the body and so they can be taken for testing whether Fur is a target for virulence modulation, as predicted by animal models [46]. For this reason, we investigated the antimicrobial activity of select SLN under these conditions, results are shown in Fig. 6. As expected, there was no measurable decrease in bacterial colonies at the end of the experiment for SLN lacking TFD (C-Chol, C-TP and C-TPAP) over a wide range of concentrations of SLN (0.975 to 1000 μg/mL PC) comparing with untreated control. In contrast, noticeable antibacterial activity was seen for the other three SLN formulations, with plots showing a $>$ 2 log reduction in surviving bacterial at concentrations above 200 μg /mL PC with MIC values of 15.6 μg/mL for C-ON-C-Chol (corresponding to 0.07 μg/mL of TFD and 0.44 μg/mL of THA respectively), 3.9 μg/mL for C-ON-C-TP (corresponding to 0.02 μg/mL of TFD and 0.12 μg/mL of THA) respectively and 3.9 μg/mL for ON-C-TPAP (corresponding to 0.02 μg/mL of TFD).

These special conditions allowed the measurement of TFD specific contribution because no TFD-mediated killing was observed under aerobic conditions, because Fur is not an essential transcription factor and the anti-bacterial activity observed was due to the contribution of THA (Table S2). Interestingly, in anaerobic conditions MIC values were much lower than in aerobic experiments. In terms of PC, it can be noticed that the MIC of SLN containing THA went from 22 to 15.6 μg /mL in C-ON-C-Chol, and from 39 to 3.9 μg /mL in C-ON-C-TP with a surprising 10 fold reduction. TFD contribution was stronger in C-ON-C-TP than in C-ON-C-Chol most likely due to the higher intracellular release of TFD, as previously confirmed by confocal microscopy (Fig. 5F′).

Even more strikingly, when ON-C-TPAP SLN were used in aerobic conditions no significant antibacterial activity was observed because no THA was present. However, when incubating the bacteria in anaerobic conditions MIC dropped from 700 μg /mL to 3.9 μg /mL of PC, the same value observed for C-ON-C-TP SLN. These results are again in accordance with confocal microscopy analysis, which showed a high TFD intracellular signal in bacteria incubated with ON-C-TPAP (Fig. 5I and I′). These data further demonstrate the specific action of TFD when they are efficiently released from SLN inside bacteria.

In order to further confirm whether the antibacterial activity was due to the specific action of the TFD inhibiting Fur activity, a comparative study was performed with C-TPAP SLN loaded with a scrambled version of the Fur TFD, referred to as Scr Fur HP TFD (See Supplementary Materials). This has the same nucleotide content of the Fur HP TFD, and will similarly form a double-stranded hairpin structure but has been designed to occupy the binding site for the Fur transcription factor to render it inert. Under microanaerobic conditions no discernable antibacterial activity was detected, with no more than 1-log reduction in CFU/mL detected for the highest concentration tested, which was 1000 ug/mL PC (See Supplementary results, Fig. S11).

3.6. In vitro and in vivo cytotoxicity studies

3.6.1. SLN cytotoxicity evaluation by MTT assay

Mindful of the need to consider the biocompatibility of any experimental antibacterial, SLN formulations were assessed for toxicity using the MTT assay using one gastrointestinal and one lung epithelial

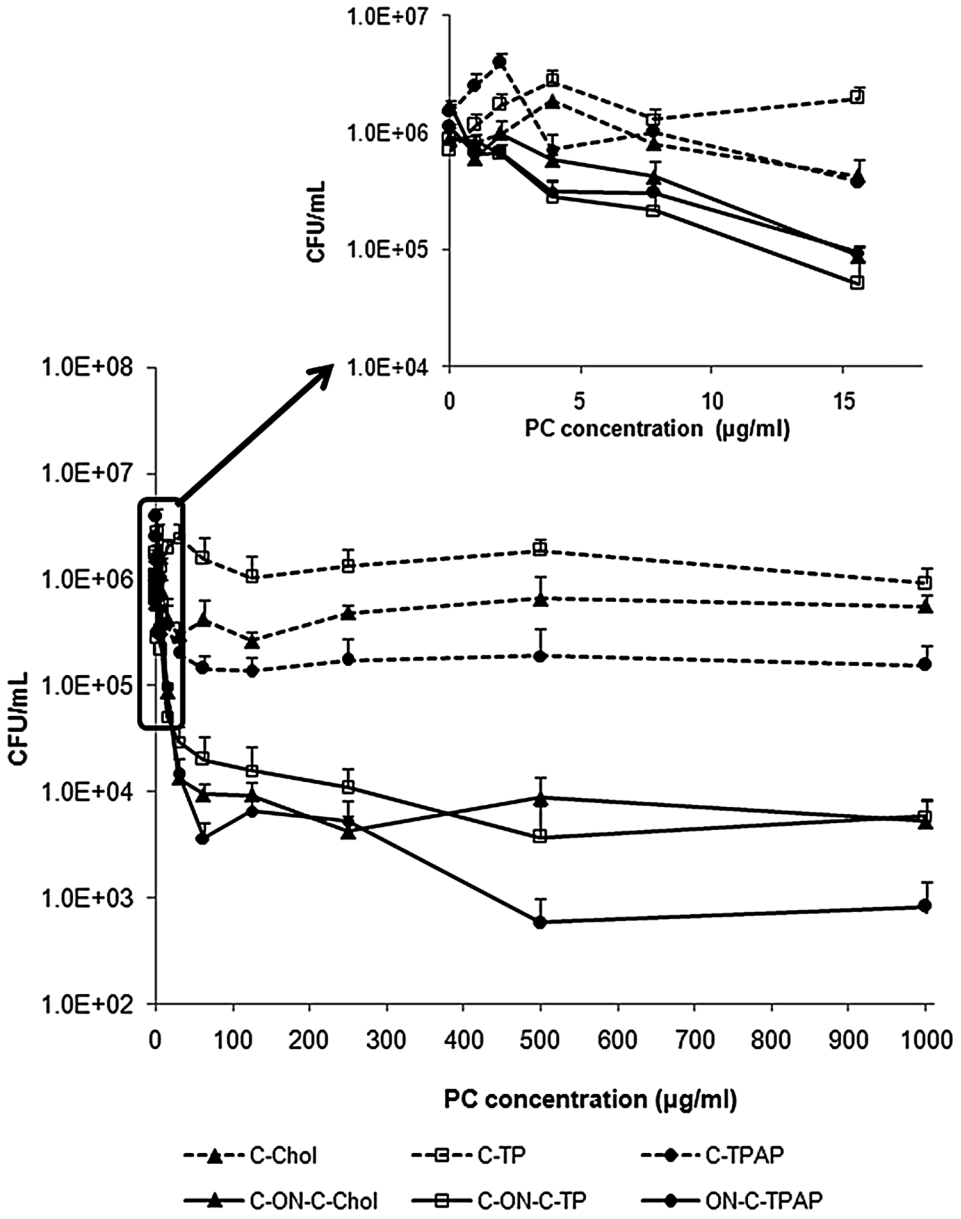

Fig. 6. Antimicrobial properties of TFD loaded SLN. The number of surviving *E. coli* colonies (CFU/mL) were counted following growth in microaerobic conditions in a minimal media supplemented with 10 µM $FeSO_4$ and 2 mM nitrate at 37 °C for a 16 h period. The media contained varying concentrations of SLN as reported by PC concentration (µg/mL). Starting inoculum was 1×10^6 CFU/mL.

cell line as models of two frequent infection sites. The IC_{50} values obtained in both cellular lines Caco-2 and Calu-3 for SLN formulations tested are summarized in Table 5 (cell viability vs. concentration plots are available in supplementary material, Fig. S12). The IC_{50} values are reported in PC units (mg/mL) and THA units (µg/mL), for comparison between SLN formulations, protamine concentrations (µg/mL) are reported for SLN not containing THA (Table 5). Results show that A-Chol and A-TP (anionic) caused no decrease in the extent of MTT turnover in Caco-2 or Calu-3 cell lines, either after 24 h or 48 h. On the other hand, C-ON-C-Chol and C-ON-C-TP (both containing THA and TFD) showed the lowest IC_{50} values in both cell lines and time points assessed. Finally, A-TPAP and ON-C-TPAP showed similar IC_{50} values despite their opposite charges; ON-C-TPAP was markedly less cytotoxic than cationic analogues C-ON-C-Chol and C-ON-C-TP (THA double layer).

Overall, IC_{50} values from MTT assays were much higher than MIC values. This selectivity for bacterial activity over mammalian toxicity ranged from 4 to 12 times for C-ON-C-Chol, 23–100 times for C-ON-C-TP and > 175 times in the case of ON-C-TPAP.

3.6.2. *In vivo toxicity of SLN on Xenopus laevis embryo model assay*

The *Xenopus laevis* larvae model was used to assess the toxicity of SLN formulations in order to obtain a robust toxicity profile of anionic and cationic SLN. This model has been previously proposed as a suitable high throughput screening model to fill the gap between the *in vitro* and *in vivo* mammalian toxicity models [31,47,48].

The cumulative percentage survival of stage 45 embryos after 96 h exposure to different SLN is shown in Fig. 7. At concentrations of 46.8 µg/mL PC no effect on larvae survival was observed. At higher concentrations (starting from 187.5 µg/mL of PC), > 10 times the MIC, these SLN reduced larval survival (42% for C-ON-C-Chol and 24% for C-ON-C-TP), which is related only to the presence of THA (Fig. 7). For SLN bearing cationic charge by virtue of a protamine coating, larvae survival was only compromised after exposure to the highest tested dose (1500 µg/mL PC). This whole organism toxicity is unlikely attributable to particle cationic charge, as the corresponding anionic SLN showed a very similar toxicity profile. Specifically, the negatively charged A-Chol and A-TP SLN caused almost no effect on the larvae

Table 5
Cytotoxicity - IC_{50} values obtained for SLN formulations incubated with Caco-2 and Calu-3 cells for 24 h and 48 h (Data represent means ± SD of three independent experiments).

Samples	IC_{50}				
	SLN component (concentration)	Caco-2		Calu-3	
		24 h	48 h	24 h	48 h
A-Chol	PC (mg/mL)	n.d.	n.d.	n.d.	n.d.
C-ON-C-Chol	PC (mg/mL)	0.18 ± 0.07	0.10 ± 0.03	0.10 ± 0.07	0.06 ± 0.05
	THA (μg/mL)	*6.23 ± 0.86*	*3.93 ± 2.11*	*4.15 ± 3.54*	*2.74 ± 2.93*
A-TP	PC (mg/mL)	n.d.	n.d.	n.d.	n.d.
C-ON-C-TP	PC (mg/mL)	0.39 ± 0.14	0.21 ± 0.08	0.11 ± 0.07	0.09 ± 0.01
	THA (μg/mL)	*17.22 ± 6.92*	*8.98 ± 3.39*	*4.83 ± 3.17*	*3.91 ± 0.18*
A-TPAP	PC (mg/mL)	n.d.	1.00 ± 0.27	0.84 ± 0.21	0.87 ± 0.17
ON-C-TPAP	PC (mg/mL)	3.07 ± 0.77	1.10 ± 0.27	0.68 ± 0.41	0.89 ± 0.12
	Prot (μg/mL)	*130.2 ± 30.6*	*47.1 ± 12.2*	*29.6 ± 18.3*	*37.8 ± 4.9*

n.d. IC_{50} not determined.

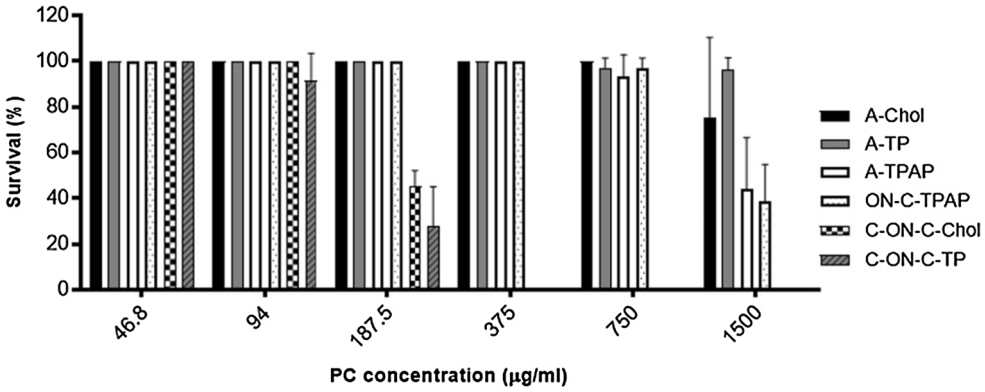

Fig. 7. *Xenopus laevis* nanotoxicity assay after exposure to A-Chol, A-TP, A-TPAP, ON-C-TPAP, C-ON-C-Chol and C-ON-C-TP: *Xenopus laevis* larvae survival after SLN exposure from stage 38 to stage 45 at 18 °C (n = 30 for each concentration).

survival even after incubation with the highest concentration (1500 μg/mL PC) at the assessed stages (from stage 38 to stage 45).These results are consistent with the toxicity trends observed by MTT assay.

Representative images of the embryos exposed to SLN at 187.5 μg/mL of PC are shown in supplementary material (Fig. S13). All embryos show the same phenotype as the control with the exception of the C-ON-C-Chol and C-ON-C-TP treated embryos which were morphologically affected by the SLN. The majority of the abnormalities observed were stunted growth/development and bent spine.

4. Conclusions

This work describes a number of formulations of cationic coated SLN for the association, protection and delivery of antimicrobial oligonucleotides (TFD) as an alternative solution to the increasing health threat of antimicrobial resistances. Beyond this, the data reported here underlines the possibility of obtaining complexes between TFD and several cationic SLN differing in the nature of the cationic coating (THA, protamine) which displayed robust DNA interaction that afforded DNAse protection *in vitro*. Moreover, the interaction between TFD-SLN complexes and bacteria showed effective TFD intracellular delivery and specific antibacterial activity under Fe limiting conditions, showing a good safety profile to eukaryotic cells at the concentrations needed for antibacterial activity. Although obtained results require further investigation, mainly to test efficacy in pathogenic bacteria strains, this work demonstrates the possibility of creating a good interaction between cationic lipid nanocarriers and oligonucleotides and supports the potentiality of such new approaches to fight drug resistance in bacteria.

Conflict of interest

The authors declare no conflict of interest in the present work.

Acknowledgements

The research leading to these results has received funding from the European Union Programme FP7-people-2013-IAPP, under the project DNA-TRAP (Grant Agreement 612338).

We would like to thank Prof Candido Pirri and Salvatore Guastella (DISAT, Polytechnic of Turin, Italy) for FESEM pictures, Giovanna Riccio, Francesco Barbero and Nanovector team for supporting HPLC analysis and for their technical advice, Dr.Alejandro Marín-Menéndez and Teresa Díaz-Calvo (Procarta Biosystems) for preliminary confocal studies and Dr. Carl Webster (University of East Anglia, UK) for his help with some experiments.

Appendix A. Supplementary material

Supplementary data to this article can be found online at https://doi.org/10.1016/j.ejpb.2018.11.017.

References

[1] R.I. Aminov, A brief history of the antibiotic era: lessons learned and challenges for the future, Front. Microbiol. 1 (2010) 134–145.
[2] K. Bush, P. Courvalin, G. Dantas, J. Davies, B. Eisenstein, P. Huovinen, G.A. Jacoby, R. Kishony, B.N. Kreiswirth, E. Kutter, S.A. Lerner, S. Levy, K. Lewis, O. Lomovskaya, J.H. Miller, S. Mobashery, L.J.V. Piddock, S. Projan, C.M. Thomas, A. Tomasz, P.M. Tulkens, T.R. Walsh, J.D. Watson, J. Witkowski, W. Witte,

G. Wright, P. Yeh, H.I. Zgurskaya, Tackling antibiotic resistance, Nat. Rev. Micro 9 (2011) 894–896.
[3] K. Lewis, Platforms for antibiotic discovery, Nat. Rev. Drug Discov. 12 (2013) 371–387.
[4] J.P. Hegarty, D.B. Stewart, Advances in therapeutic bacterial antisense biotechnology, App. Microb. Biotech. 102 (2018) 1055–1065.
[5] E.K. Sully, B.L. Geller, Antisense antimicrobial therapeutics, Curr. Opin. Microbiol. 33 (2016) 47–55.
[6] A.R. Gascon, A.d. Pozo-Rodriguez, M.A. Solinis, Non-viral delivery systems in gene therapy, Gene Therapy – Tools Potential Appl. (2013).
[7] B. Hui, X. Xiaoyan, H. Zheng, Z. Ying, M. Jingru, L. Xiaoxing, Antisense antibiotics: a brief review of novel target discovery and delivery, Curr. Drug Discov. Technol. 7 (2010) 76–85.
[8] G. McClorey, S. Banerjee, Cell-penetrating peptides to enhance delivery of oligonucleotide-based therapeutics, Biomedicines 6 (2018) 51.
[9] T. Lehto, K. Ezzat, M.J.A. Wood, S. El Andaloussi, Peptides for nucleic acid delivery, Adv. Drug Deliv. Rev 106 (Part A) (2016) 172–182.
[10] X.-Y. Xue, X.-G. Mao, Y. Zhou, Z. Chen, Y. Hu, Z. Hou, M.-K. Li, J.-R. Meng, X.-X. Luo, Advances in the delivery of antisense oligonucleotides for combating bacterial infectious diseases, Nanomed. Nanotech. 14 (2018) 745–758.
[11] J.P. Hegarty, J. Krzeminski, A.K. Sharma, D. Guzman-Villanueva, V. Weissig, D.B. Stewart Sr., Bolaamphiphile-based nanocomplex delivery of phosphorothioate gapmer antisense oligonucleotides as a treatment for Clostridium difficile, Int. J. Nanomed. 11 (2016) 3607–3619.
[12] A. Marín-Menéndez, C. Montis, T. Díaz-Calvo, D. Carta, K. Hatzixanthis, C.J. Morris, M. McArthur, D. Berti, Antimicrobial nanoplexes meet Model Bacterial Membranes: the key role of Cardiolipin, Sci. Rep. 7 (2017) 41242.
[13] M. Mamusa, L. Sitia, F. Barbero, A. Ruyra, T.D. Calvo, C. Montis, A. Gonzalez-Paredes, G.N. Wheeler, C.J. Morris, M. McArthur, D. Berti, Cationic liposomal vectors incorporating a bolaamphiphile for oligonucleotide antimicrobials, Biochim. Biophys. Acta Biomembr. 2017 (1859) 1767–1777.
[14] M. Bondi, E. Craparo, Solid lipid nanoparticles for applications in gene therapy: a review of the state of the art, Exp. Opin. Drug Deliv. 7 (2010) 7–18.
[15] A. del Pozo-Rodriguez, D. Delgado, M.A. Solinis, A.R. Gascon, Lipid nanoparticles as vehicles for macromolecules: nucleic acids and peptides, Recent Pat. Drug Deliv. Formul. 5 (2011) 214–226.
[16] C. Musicanti, P. Gasco, Solid Lipid-Based Nanoparticles, in: B. Bhushan (Ed.) Encyclopedia of Nanotechnology, Springer Netherlands: Dordrecht, 2012, p. 2487-2487.
[17] R. Cortesi, M. Campioni, L. Ravani, M. Drechsler, M. Pinotti, E. Esposito, Cationic lipid nanosystems as carriers for nucleic acids, New Biotechnol. 31 (2014) 44–54.
[18] A.M. Brioschi, S. Calderoni, L.G. Pradotto, M. Guido, A. Strada, F. Zenga, C.A. Benech, F. Benech, L. Serpe, G.P. Zara, C. Musicanti, A. Ducati, M.R. Gasco, A. Mauro, Solid lipid nanoparticles carrying oligonucleotides inhibit vascular endothelial growth factor expression in rat glioma models, J. Nanoneurosci. 1 (2009) 65–74.
[19] K. Tabatt, C. Kneuer, M. Sameti, C. Olbrich, R.H. Müller, C.-M. Lehr, U. Bakowsky, Transfection with different colloidal systems: comparison of solid lipid nanoparticles and liposomes, J. Control. Release. 97 (2004) 321–332.
[20] A. del Pozo-Rodríguez, D. Delgado, M.Ã. Solinís, J.L. Pedraz, E. Echevarría, J.M. Rodríguez, A.R. Gascón, Solid lipid nanoparticles as potential tools for gene therapy: In vivo protein expression after intravenous administration, Int. J. Pharm. 385 (2010) 157–162.
[21] D. Delgado, A.R. Gascon, A. del Pozo-Rodriguez, E. Echevarria, A.P. Ruiz de Garibay, J.M. Rodriguez, M.A. Solinis, Dextran-protamine-solid lipid nanoparticles as a non-viral vector for gene therapy: In vitro characterization and in vivo transfection after intravenous administration to mice, Int. J. Pharm. 425 (2012) 35–43.
[22] M. McArthur, Transcription factor decoys for the treatment and prevention of infections caused by bacteria including Clostridium difficile. US Patent App. 13/802, 103, 2013.
[23] S.W. Seo, D. Kim, H. Latif, E.J. O'Brien, R. Szubin, B.O. Palsson, Deciphering Fur transcriptional regulatory network highlights its complex role beyond iron metabolism in Escherichia coli, Nat. Commun. 5 (2014).
[24] M.R. Gasco, L. Priano, G.P. Zara, S. Hari Shanker, Solid lipid nanoparticles and microemulsions for drug delivery: The CNS, in Progress in Brain Research, Elsevier, 2009, pp. 181–192 (Chapter 10).
[25] E. Ugazio, R. Cavalli, M.R. Gasco, Incorporation of cyclosporin A in solid lipid nanoparticles (SLN), Int. J. Pharm. 241 (2002) 341–344.
[26] ICH, guideline Q3C (R6) on impurities: guideline for residual solvents, Eur. Med. Agency (2016).
[27] M. Ruponen, S. Ylä-Herttuala, A. Urtti, Interactions of polymeric and liposomal gene delivery systems with extracellular glycosaminoglycans: physicochemical and transfection studies, Biochim. Biophys. Acta Biomembr. 1415 (1999) 331–341.
[28] F. Cockerill, Methods for dilution antimicrobial susceptibility tests for bacteria that grow aerobically, Clinical and Laboratory Standard Institute, 2012.
[29] European Committee for Antimicrobial Susceptibility Testing of the European Society of Clinical, M. and D. Infectious, Determination of minimum inhibitory concentrations (MICs) of antibacterial agents by broth dilution. Clin. Microbiol. Infect. 9 (2003) ix-xv.
[30] I. Wiegand, K. Hilpert, R.E. Hancock, Agar and broth dilution methods to determine the minimal inhibitory concentration (MIC) of antimicrobial substances, Nat. Protoc. 3 (2008) 163–175.
[31] K. Al-Yousuf, C.A. Webster, G.N. Wheeler, F.B. Bombelli, V. Sherwood, Combining Cytotoxicity Assessment and Xenopus laevis Phenotypic Abnormality Assay as a Predictor of Nanomaterial Safety, in: Current Protocols in Toxicology, 2017, John Wiley & Sons, Inc.
[32] L. Benedini, S. Antollini, M.L. Fanani, S. Palma, P. Messina, P. Schulz, Study of the influence of ascorbyl palmitate and amiodarone in the stability of unilamellar liposomes, Mol. Membr. Biol. 31 (2014) 85–94.
[33] V. Teeranachaideekul, R.H. Müller, V.B. Junyaprasert, Encapsulation of ascorbyl palmitate in nanostructured lipid carriers (NLC)-effects of formulation parameters on physicochemical stability, Int. J. Pharm. 340 (2007) 198–206.
[34] J.V. González-Aramundiz, E. Presas, I. Dalmau-Mena, S. Martínez-Pulgarín, C. Alonso, J.M. Escribano, M.J. Alonso, N.S. Csaba, Rational design of protamine nanocapsules as antigen delivery carriers, J. Control. Release. 245 (2017) 62–69.
[35] A. del Pozo-Rodríguez, D. Delgado, M.A. Solinís, A.R. Gascón, J.L. Pedraz, Solid lipid nanoparticles: formulation factors affecting cell transfection capacity, Int. J. Pharm. 339 (2007) 261–268.
[36] H.Q. Mao, K. Roy, V.L. Troung-Le, K.A. Janes, K.Y. Lin, Y. Wang, J.T. August, K.W. Leong, Chitosan-DNA nanoparticles as gene carriers: synthesis, characterization and transfection efficiency, J. Control. Release. 70 (2001) 399–421.
[37] M. Mamusa, F. Barbero, C. Montis, L. Cutillo, A. Gonzalez-Paredes, D. Berti, Inclusion of oligonucleotide antimicrobials in biocompatible cationic liposomes: a structural study, J. Colloid Interf. Sci. 508 (2017) 476–487.
[38] M. Mamusa, C. Resta, F. Barbero, D. Carta, D. Codoni, K. Hatzixanthis, M. McArthur, D. Berti, Interaction between a cationic bolaamphiphile and DNA: The route towards nanovectors for oligonucleotide antimicrobials, Colloids Surf. B. 143 (2016) 139–147.
[39] D. Delgado, A. del Pozo-Rodríguez, M.A. Solinís, A. Rodríguez-Gascón, Understanding the mechanism of protamine in solid lipid nanoparticle-based lipofection: the importance of the entry pathway, Eur. J. Pharm. Biopharm. 79 (2011) 495–502.
[40] S.-N. He, Y.-L. Li, J.-J. Yan, W. Zhang, Y.-Z. Du, H.-Y. Yu, F.-Q. Hu, H. Yuan, Ternary nanoparticles composed of cationic solid lipid nanoparticles, protamine, and DNA for gene delivery, Int. J. Nanomed. 8 (2013) 2859–2869.
[41] H. Yuan, W. Zhang, Y.-Z. Du, F.-Q. Hu, Ternary nanoparticles of anionic lipid nanoparticles/protamine/DNA for gene delivery, Int. J. Pharm. 392 (2010) 224–231.
[42] C. Gottstein, G. Wu, B.J. Wong, J.A. Zasadzinski, Precise quantification of nanoparticle internalization, ACS Nano 7 (2013) 4933–4945.
[43] L. Sitia, R. Ferrari, M.B. Violatto, L. Talamini, L. Dragoni, C. Colombo, L. Colombo, M. Lupi, P. Ubezio, M. D'Incalci, M. Morbidelli, M. Salmona, D. Moscatelli, P. Bigini, Fate of PLA and PCL-based polymeric nanocarriers in cellular and animal models of triple-negative breast cancer, Biomacromolecules 17 (2016) 744–755.
[44] L. Sitia, K. Paolella, M. Romano, M.B. Violatto, R. Ferrari, S. Fumagalli, L. Colombo, E. Bello, M.G. De Simoni, M. D'Incalci, M. Morbidelli, E. Erba, M. Salmona, D. Moscatelli, P. Bigini, An integrated approach for the systematic evaluation of polymeric nanoparticles in healthy and diseased organisms, J. Nanop. Res. 16 (2014) 2481.
[45] T. Wang, J. Bai, X. Jiang, G.U. Nienhaus, Cellular uptake of nanoparticles by membrane penetration: a study combining confocal microscopy with FTIR spectroelectrochemistry, ACS Nano 6 (2012) 1251–1259.
[46] K. Hantke, Iron and metal regulation in bacteria, Curr. Opin. Microbiol. 4 (2001) 172–177.
[47] B. Akache, F.C. Stark, U. Iqbal, W. Chen, Y. Jia, L. Krishnan, M.J. McCluskie, Safety and biodistribution of sulfated archaeal glycolipid archaeosomes as vaccine adjuvants, Hum. Vacc. Immunother. (2018) 1–14.
[48] C.A. Webster, D. Di Silvio, A. Devarajan, P. Bigini, E. Micotti, C. Giudice, M. Salmona, G.N. Wheeler, V. Sherwood, F.B. Bombelli, An early developmental vertebrate model for nanomaterial safety: bridging cell-based and mammalian toxicity assessment, Nanomedicine 11 (2016) 643–656.